MRI and PET of Brain Tumor Neuroinflammation in the Era of Immunotherapy, From the *AJR* Special Series on Inflammation

Cymon N. Kersch, MD, PhD[1], **Prakash Ambady, MD**[2], **Bronwyn E. Hamilton, MD**[3], **Ramon F. Barajas Jr., MD**[3,4,5]

[1]School of Medicine, Oregon Health and Science University, Portland, OR.

[2]Department of Neurology, Oregon Health and Science University, Portland, OR.

[3]Department of Radiology, Neuroradiology Section, Oregon Health and Science University, 3181 SW Sam Jackson Park Rd, Portland, OR 97239.

[4]Advanced Imaging Research Center, Oregon Health and Science University, Portland, OR.

[5]Knight Cancer Institute, Oregon Health and Science University, Portland, OR.

Abstract

With the emergence of immune-modulating therapies, brain tumors present important diagnostic imaging challenges. These challenges include planning personalized treatment and adjudicating accurate monitoring approaches and therapeutically specific response criteria. The challenges have been due, in part reliance on nonspecific imaging metrics, such as gadolinium contrast-enhanced MRI or FDG PET, and rapidly evolving biologic understanding of neuroinflammation. The importance of the tumor immune interaction and ability to therapeutically augment inflammation to improve clinical outcomes make it necessary for radiologists to develop a working knowledge of the immune system and its role in clinical neuroimaging. The purpose of this article is to review relevant biologic concepts of the tumor microenvironment of primary and metastatic brain tumors, the interactions between the tumors and the immune system, and MRI and PET methods for imaging inflammatory elements associated with these malignancies. In recognition of the growing fields of immunotherapeutics and precision oncology, clinically translatable imaging metrics for the diagnosis and monitoring of brain tumor neuroinflammation are highlighted. Practical guidance is provided for implementing iron nanoparticle imaging, including imaging indications, protocols, interpretation, and pitfalls. A comprehensive understanding of the inflammatory mechanisms within brain tumors and their imaging features will facilitate the development of innovative noninvasive prognostic and predictive imaging strategies for precision oncology.

Keywords

ferumoxytol; glioblastoma; inflammation; metastasis; MRI

Importance of Imaging of Neuroinflammation in the Era of Immunotherapy and Precision Oncology

Neurooncology has entered an exciting phase of cutting-edge treatments that integrate targeting of tumor-specific inflammation and unique protein alterations, termed precision oncology [1]. Critical challenges remain in bringing the precision oncology paradigm to neurooncology, including adjudicating accurate monitoring approaches and specific therapeutic response criteria. Neuroimaging has the potential to help overcome these challenges. The brain tumor–immune interface is central to these new interventions. Immunotherapies directly target specific immune components or their interactions within the tumor immune microenvironment. The biologic sequelae of immunotherapy directly influence clinical imaging phenotypes, necessitating better understanding of the inflammatory elements associated with neuroimaging characteristics. A comprehensive understanding of the inflammatory mechanisms within brain tumors and their imaging features fosters the development of innovative noninvasive prognostic and predictive imaging strategies for use in precision oncology.

In this article, we review the tumor microenvironment of primary and metastatic brain tumors, interactions between these tumors and the immune system, and clinically applicable methods for imaging elements of brain tumor neuroinflammation.

Active Immune Component of the Tumor Environment in Primary and Metastatic CNS Malignancies

The CNS was long considered an immune-privileged site, protected from systemic inflammation by the blood-brain barrier. The CNS is now recognized to harbor resident cells with immunologic functions that constitute a system for immune surveillance augmented by infiltrating systemic immune cells and a meningeal lymphatic system [2–6]. Within primary and metastatic brain tumors, cellular and protein immune components are important features of the brain tumor microenvironment; they influence tumor survival, growth, and treatment response. Collectively, the brain tumor microenvironment contains malignant cells, resident brain cells (including astrocytes, microglia, pericytes, and endothelial cells), and systemic immune cells (commonly macrophages and lymphocytes) [5] (Fig. 1).

Reactive astrocytes are present in and immediately surround brain tumors, where they display substantial plasticity (i.e., can change their cellular functions and physical shape) [7]. In the tumor microenvironment, some astrocytes promote tumor growth and survival by enhancing their invasive capacity or by protecting malignant cells from therapeutic and immune attack [8, 9]. Conversely, other astrocytes may exhibit antitumor effects, for instance by releasing exosomes containing micro-RNA that inhibits tumor growth [10].

Microglia, pericytes, and endothelial cells also influence tumor growth and neuroinflammation, which can produce key clinical imaging features. Microglia are described later in this article. Pericytes exist on the abluminal surface of vasculature, where they affect tumor vascularization, blood-brain barrier integrity, and tumor dormancy [11, 12]. Endothelial cells form the tumor vasculature, which directly impacts tumor survival through various mechanisms [13, 14]. The endothelial cells also facilitate a tumor immune reaction by producing and secreting neuroimmune substances, including numerous cytokines that propagate neuroinflammation signaling [15].

Tumor vasculature includes previously established vasculature and neovasculature that develop in response to local hypoxia, metabolic demands, and elevated levels of vascular endothelial growth factor [14, 16]. Tumor vasculature can be abnormal in its structure and function, causing increased, but variable, permeability in brain tumors [17, 18] (Fig. 1B). Typically, the bulk tumor region has more dysfunctional vasculature, whereas peritumoral vasculature resembles normal cerebral blood vessels, as exemplified by enhancement on MRI after administration of a gadolinium-based contrast agent (GBCA) [13, 17]. IV-administered GBCAs enter the extracellular space in the brain parenchyma through leaky tumor vasculature, manifesting as regions of hyperintensity on T1-weighted MR images. Importantly, nonenhancing regions of brain surrounding areas of enhancement can exhibit tumor cells histologically, highlighting that the presence or absence of tumor cells does not directly correlate with blood-brain barrier leakiness [19].

Clinically Relevant Interactions Between the Immune System and Brain Tumors

The brain has unique immune monitoring mechanisms, including a meningeal lymphatic vessel, a parenchymal glymphatic pathway, a system for immune cell surveillance, and a resident CNS phagocytic cell population (i.e., microglia) [2, 5, 20].

Microglia and macrophages can account for more than 30% of the bulk tumor mass and play key roles in tumor progression [3, 9, 21]. Microglia migrate to the brain from yolk sac precursor cells in embryonic development to form a self-propagating resident phagocytic cell population [22]. Macrophages migrate to the brain throughout life from circulating bone marrow–derived monocytes. Collectively, microglia and macrophages associated with malignancies are termed tumor-associated macrophages (TAMs). Approximately 85% of TAMs in glioblastomas are from the systemic circulation [23]. Lineage-tracing experiments in brain metastases have shown that both microglia and bone marrow–derived monocytes infiltrate these tumors [24].

TAMs in brain tumors can activate into a spectrum of proinflammatory (M1) to antiinflammatory (M2) macrophage phenotypes that influence the inflammatory cascade, lymphocyte activation, angiogenesis and vascular function, tissue remodeling, treatment sensitivity, and tumor survival [5, 24–28] (Fig. 1C). Although the M1/M2 bipolarization model likely operates as ends of a spectrum, it provides a framework to conceptualize their multifaceted roles [29]. M1 macrophages characteristically function in pathogen and tumor killing. In comparison, M2 macrophages function to contain and resolve inflammatory

reactions and thus can promote tumor survival by blunting the activity of cytotoxic immune cells [27, 30].

A dysregulated adaptative immune response within the tumor microenvironment also contributes to cell survival. The functional and prognostic roles of these cells are an area of ongoing research. For instance, CD8+ T-cell infiltrates in glioblastoma have been associated with prolonged patient survival, whereas regulatory T cells have been correlated with worse prognosis despite their limited presence [31].

The ability of the immune system to function in tumor control is greatly influenced by immune checkpoints. Physiologically, immune checkpoints inhibit immune responses to self-antigens. Many neoplasms, including CNS tumors and metastases, use this mechanism to prevent immune cells from recognizing and mounting an inflammatory response [32].

Immunotherapies target the tumor immune interaction. Such therapies include immune checkpoint modulators, engineered chimeric antigen receptor (CAR) T cells, oncolytic viral vectors, and vaccines (Fig. 2). Immune checkpoint inhibition and vaccines are thought to primarily function therapeutically by means of disinhibiting T-cell activation. Vaccine-based immunotherapies entail the use of tumor-associated antigens to train the immune system to target tumor cells through various immune mechanisms in an effort to induce cytotoxic tumor effects. Tumor antigens are presented to antigen-presenting immune cells, such as dendritic cells, ex vivo. These cells are then administered to the patient, inducing a potent adaptive immune stimulus. Thus, cell populations in both the innate and adaptive arms of the immune system may be therapeutically mobilized to increase immune-mediated tumor cell death.

Methods for Imaging Brain Tumor Inflammation

The workhorses of biologically specific noninvasive assessment of neuroinflammation are MRI, PET, and SPECT. These modalities yield information about neuroinflammation through labeling of cells and molecules that have immune function, evaluation of blood-brain barrier breakdown based on contrast agent leakage, identification of the consequences of neuroinflammation, and association of phenotypic imaging patterns with inflammatory genomic or transcriptomic patterns, a technique broadly termed imaging genomics.

Practical Guide for Implementing Iron Nanoparticle Contrast-Enhanced MRI

Directly labeling key immune cells is a rapidly developing area of neuroinflammation imaging (Fig. 1D). Most work in brain tumor–associated neuroinflammation has focused on labeling TAMs. Because MRI is integral to clinical brain tumor evaluation and monitoring, novel methods of applying MRI-based neuroinflammation imaging are readily adaptable to clinical practice.

Indications for Use of Iron Nanoparticle Contrast Agents

In CNS malignancies, GBCAs are used to differentiate areas with varying contrast dynamics (i.e., blood-brain barrier leakage) to identify bulk tumor. Alternatively, contrast agents such as ultrasmall superparamagnetic iron oxide (USPIO) nanoparticles have

added ability to capture inflammation because such agents can be taken up by cells with phagocytic functions. One such agent is ferumoxytol (Feraheme, AMAG), a 17- to 31-nm USPIO nanoparticle [33, 34]. Ferumoxytol-enhanced MRI is actively being studied in pediatric and adult brain tumors to evaluate its safety and imaging properties (clinicaltrials.gov identifiers NCT00978562, NCT00103038, NCT00660543, NCT00659126, NCT00769093, and NCT00659776). Ferumoxytol traffics preferentially to reactive lesions during inflammation. In a rodent brain model, ferumoxytol was present 24 hours after delivery in reactive astrocyte end feet and in CD163+/CD68+ microglia and macrophages [35, 36]. Importantly, in this model, ferumoxytol was not taken up by the tumor cells. This finding highlights the utility of delayed ferumoxytol-enhanced MRI performed 24 hours after infusion as a method to identify a reactive immune component of brain tumors.

The use of ferumoxytol as an MRI contrast agent is off label from the approved clinical indication. Ferumoxytol is currently FDA approved for the treatment of iron deficiency anemia in adults who are intolerant of or whose condition is medically refractory to oral therapy or who have chronic kidney disease. However, ferumoxytol has been used as an alternative contrast agent in clinical scenarios in which GBCA administration is contraindicated, including renal failure and medically refractory life-threating GBCA allergy. This usage pattern is noninferior to use of GBCAs for the detection of primary and metastatic brain tumors [37, 38].

Iron Nanoparticle MRI Protocol

Ferumoxytol has been studied as an MRI contrast agent at doses ranging from 1 to 11 mg/kg, with a total dose up to 510 mg. Immediately after IV infusion, ferumoxytol serves as a blood pool contrast agent (Fig. 3). Use of T2*-based dynamic susceptibility-weighted contrast-enhanced technique allows quantification of perfusion metrics, such as cerebral blood volume (CBV). The absence of marked brain vascular leakage allows acquisition of high-resolution CBV maps by means of steady-state T2*-weighted or susceptibility-weighted technique without sophisticated leakage correction mathematic modeling.

The use of ferumoxytol as an MRI contrast agent to assess neuroinflammation has potential biologic advantages over use of a GBCA. Ferumoxytol has a 14- to 21-hour plasma half-life. This prolonged circulating time allows localization within the brain tumor interstitial space through intracellular trafficking of the iron nanoparticles within TAMs or through slow leakage from the neovascular space and subsequent phagocytosis. Irrespective of the mechanism, brain parenchymal MRI signal changes within regions of tumor-associated neuroinflammation maximally occur within 48 hours of IV administration (Fig. 3). Typically, ferumoxytol induces T1, T2, and T2* shortening within sites of neuroinflammation (Fig. 4).

We have found a ferumoxytol dose of 4–7 mg/kg (to a total dose of 510 mg) sufficient for assessment of brain tumor vascularity and neuroinflammatory characteristics. A ferumoxytol dose of 1 mg/kg achieves quality similar to that of MRA performed with a clinical dose of GBCA [34]. Nonetheless, the signal-to-noise ratio at a dose of 2 mg/kg may be insufficient for generation of dynamic susceptibility contrast images or a steady-state CBV map [39].

Practically, assessment of brain tumor neuroinflammation requires imaging in the delayed phase 24–48 hours after prior ferumoxytol administration if recent unenhanced T1-weighted imaging has been performed. Multiple consensus recommendations describe techniques that are compliant with the standardized brain tumor imaging protocol [40–43]. A brain tumor imaging protocol–compliant ferumoxytol contrast-enhanced MRI protocol is provided in Table 1.

Interpretation of Iron Nanoparticle Contrast-Enhanced MRI

Interpretation of T1-weighted ferumoxytol contrast-enhanced MRI appears to depend on the clinical context. Before chemoradiotherapy, primary and metastatic brain tumors have similar characteristics on GBCA- and ferumoxytol-enhanced images [34, 38, 44] (Fig. 4). However, the enhancing features are dissimilar in patients with therapy-induced neuroinflammation. Immunotherapies can elicit a neuroinflammatory effect that results in increased gadolinium enhancement and T2 hyperintensity on MRI, appearing similar to tumor growth but subsequently undergoing spontaneous regression (Fig. 5). This imaging pattern, termed pseudoprogression, is observed in approximately 30% of patients with glioblastoma undergoing chemoradiotherapy and is now seen in patients treated with immune checkpoint inhibitors [45]. Given the mechanism of action, the incidence of immunotherapeutically induced neuroinflammatory changes may be higher with immunotherapies than with standard chemoradiation. The clinical significance of pseudoprogression remains debated, though pseudoprogression may be associated with improved survival [46]. Thus, differentiating pseudoprogression from tumor growth is critical for clinical decision-making. An extensive body of literature [47–50] describes the use of perfusion-weighted imaging for the differentiation of these two processes. Meta-analyses [51–53] provide evidence that the use of biologically nonspecific imaging metrics as surrogate markers of neuroinflammation may be clinically limited; for example, CBV has pooled sensitivity and specificity that are both approximately 80%. However, strong evidence indicates that physiologic metrics such as CBV improve on qualitative metrics, such as contrast enhancement, which performs considerably worse (e.g., pooled sensitivity of 68% and specificity of 77% [51]).

To address the shortcomings of gadolinium-based response criteria for patients with brain tumors undergoing immunotherapy, the Response Assessment for Neuro-Oncology Working Group published the Immunotherapy Response Assessment in Neuro-Oncology guidelines in 2015 [54]. Use of these guidelines may be difficult when new or progressively enhancing lesions develop in a patient who has no symptoms. If the patient started immunotherapy more than 6 months previously, the imaging changes are presumed to represent disease progression. If the patient is less than 6 months from initiation of immunotherapy, the change in enhancement is considered equivocal. The MRI examination showing initial radiologic progression becomes the new baseline examination, and follow-up MRI 1–3 months later is recommended. Treatment failure and inflammation can cause similar GBCA enhancement. If the enhancement has continued to worsen at the 3-month follow-up examination, disease progression is presumed.

The diagnostic potential of imaging with USPIO nanoparticles is being assessed to differentiate pseudoprogression from tumor growth (NCT00660543) [44] (Figs. 6 and 7). Preliminary results suggest that glioblastoma pseudoprogression may be defined by disproportionate T1 shortening of the USPIO-enhancing area with respect to the corresponding GBCA-enhancing area. ROC curve analysis of the natural log of the ferumoxytol-to-GBCA sum of products diameter ratio suggests a threshold value of 0.56 (1.75 natural log ratio) in isocitrate dehydrogenase 1 (IDH1) wild-type glioblastoma as the cutoff value for the diagnosis of pseudoprogression, having 100% sensitivity and specificity in the study sample. This potential imaging biomarker of immunotherapy-associated neuroinflammation is being prospectively assessed in patients with newly diagnosed glioblastoma treated with standard-of-care and concurrent pembrolizumab administration (NCT03347617). The tracking of TAMs is also expected to be important in the context of biologically specific checkpoint inhibition directed at CD47, also known as integrin-associated protein, to improve phagocytic properties.

Iron Nanoparticle Imaging Precautions and Pitfalls

The FDA in March 2015 issued a black box warning about the risk of potential acute hypersensitivity reactions to bolus injection of undiluted ferumoxytol during therapeutic administration [55]. Seventy-nine instances of serious adverse events were reported among an estimated 1.2 million injections. The FDA issued updated recommendations for therapeutic prescription of ferumoxytol that included dilution (1:4 ratio with normal saline solution), infusion over 15 minutes, and hemodynamic monitoring for up to 30 minutes after infusion. Nguyen et al. [56] reported the positive safety profile of ferumoxytol as a diagnostic MRI contrast agent. Data in the FeraSafe multicenter MRI registry, which includes 3215 adult and pediatric patients who underwent a total of 4240 injections, suggest that the use of ferumoxytol as a diagnostic MRI contrast agent is well tolerated, is associated with no serious adverse events, and is implicated in few adverse reactions [56]. Despite this reported safety profile, it is prudent (and the FDA recommends) that ferumoxytol be administered only when personnel and therapies are immediately available for the treatment of anaphylaxis and other hypersensitivity reactions. Regardless, all MRI centers should be prepared for the treatment of the acute hypersensitivity reactions that are also observed with GBCA administration. The American College of Radiology [57] provides recommendations for the treatment of contrast reactions. In addition, Lim et al. [58] also provide expert panel consensus guidance for the management of hypersensitivity reactions to IV iron in adults (Fig. 8).

Several imaging pitfalls unique to iron nanoparticle imaging warrant mention. First, intravascular signal persists and contributes to the observed parenchymal signal at the delayed imaging time point. A prospective pilot study [59] confirmed that in adults with newly diagnosed high-grade gliomas, delayed ferumoxytol imaging captures TAMs in the tumor microenvironment. In that study, positive correlations were identified between susceptibility and relaxation rates R2*(1/T2*) and R2(1/T2) with the number of CD163- and CD68-positive macrophages found at histopathologic analysis. Although ferumoxytol-based MRI of TAMs is accomplished by imaging 24 hours after nanoparticle infusion, imaging immediately after infusion captures the nanoparticle while it is in the intravascular phase,

allowing identification of highly vascularized tissue [39]. Differentiating these intravascular from extravascular ferumoxytol pools in brain tumors is an emerging imaging tool for TAM identification. Segregation and extravascular localization of ferumoxytol imaging (SELFI) is a novel technique whereby ferumoxytol-enhanced early and delayed susceptibility-weighted imaging is used to account for persistent intravascular ferumoxytol signal and more precisely identify the TAM content of glioblastoma [60]. In addition, the radiologist should be aware of the prolonged clearance time of iron nanoparticles. Changes in ferumoxytol signal may remain present in brain abnormalities several days after administration [34]. This persistent signal change is an important diagnostic consideration during short-interval follow-up examinations, because it may be confused with early subacute blood products. Finally, decreased signal intensity in liver, spleen, and bone marrow may be observed on MRI for several months.

PET

PET has been widely studied for imaging of neuroinflammation. PET is a noninvasive molecular imaging technique that records the distribution of positron-emitting isotopes bound to select tracer molecules [61]. Tracer molecules that are specific and sensitive for immune elements, such as activated microglia and macrophages, have been the backbone of this research effort. Applying PET techniques to brain pathology has been challenged by limited PET ligand CNS bioavailability due to systemic plasma protein binding, low blood-brain barrier permeability within non–gadolinium-enhancing tumor components, and active extrusion across the cerebral vasculature. Despite these obstacles, progress has been made in this area.

The first widely studied radiotracer imaging of neuroinflammation targeted the 18-kDa protein called translator protein (TSPO), originally known as the peripheral benzodiazepine receptor [61, 62]. TSPO is a mitochondrial transmembrane protein expressed in macrophage lineage cells, including microglia, that is upregulated in response to neuroinflammation, brain injury, and CNS tumors [62–64]. TSPO expression has also been identified in reactive astrocytes, but this expression varies with neurologic insult and research model [65, 66]. TSPO may also be expressed in neoplastic glioma cells and endothelial cells [67–69]. The prototype TSPO ligand, isoquinoline carboxamide ^{11}C-PK11195, was identified in the 1990s. Since then, second- and third-generation ligands of TSPO that have higher binding affinity and that circumvent the issue of TSPO allelic variability in humans have been developed [70, 71]. This work has resulted in more than 13 unique TSPO radiotracers in five structural classes [66, 71]. TSPO ligands for use in malignant brain pathology that have improved tumor-to-background brain signal and that entail nanocarrier technology to enhance CNS bioavailability are under development [63, 72, 73]. These tracers are already showing promise in delineating clinically important neuroinflammation tumor features, such as radiation necrosis [74]. Although TSPO tracers non-invasively capture general reactive gliosis in neuroinflammation, evaluating the utility of TSPO tracers in selective imaging of polarized immunotypes remains an active area of investigation. There is evidence of TSPO upregulation in proinflammatory and immunosuppressive conditions [61, 68, 75].

PET tracers targeting additional neuroinflammatory proteins that map reactive glia can also be used in neuroinflammation imaging. These targets include monoamine oxidase B, glycogen synthase 3, cyclooxygenase-1 and −2, arachidonic acid, several arachidonic acid receptors, the nicotinic acetylcholine receptor α4β2, imidazole-2 binding sites, sphingosine-1 phosphate receptor 1, purinergic receptors ($P2X_7$ and $P2Y_{12}$), and the cannabinoid-2 receptor [61, 66]. The varied expression of these molecular targets in reactive microglia versus astrocytes has been reviewed [61]. To date, the utility of these targets in neuroinflammation imaging has been studied in nonneoplastic noninfectious brain abnormalities and has yet to be evaluated in tumors.

Whereas systemic immune cells are present in CNS malignancies, less research has been conducted on infiltrating cells such as T cells, B cells, and natural killer (NK) cells than on reactive glia and TAMs. Historically, tracking these cells was accomplished by injecting autologous leukocytes that had been incubated with a radiotracer [76]. In rodent models of nonmalignant CNS pathology, this technique has identified neutrophils, CD4+ T cells, and CD8+ T cells trafficking to inflammatory brain regions [77–79]. In a patient with recurrent high-grade glioma, this technique was used to deliver genetically engineered CD8+ cytotoxic T cells with image tracking by PET [80]. After treatment, the infused cells were visualized within the tumor, albeit not quantifiably. Advances in CAR T-cell techniques have provided new opportunities for in vivo imaging of ex vivo tagged immune cells. Keu et al. [81], in a pilot study of recurrent glioblastoma, reported on the safety and utility of PET with 9-(4-^{18}F-fluoro-3-[hydroxymethyl]butyl)guanine (^{18}F-FHBG) to longitudinally track stably transfected T cells. Theoretically, this technique applies to evaluating brain trafficking of other leukocyte populations in tumors. Tracers targeting multiple immune cells influenced by cancer immunotherapies are being developed. For instance, Shaffer et al. [82] developed and completed preclinical in vitro and in vivo validation of two antibody-based PET probes targeting a specific protein upregulated on activated NK cells. Although their study focused on renal cell carcinoma, this or similar technology could be applied to evaluating CNS malignancies.

As immunotherapies are being used and studied in oncology, novel imaging techniques are being developed to measure antigen expression, quantify drug delivery, and assess therapeutic efficacy. These techniques largely rely on labeling and imaging of molecular targets of immunotherapies and immune cell populations activated by their effects. Immunotherapy targets can be imaged with immuno-PET, a method that conjugates radionucleotides with antibodies or fragments of antibodies targeting immune constituents (Fig. 1E). Initial human studies investigating immuno-PET were conducted with the radioligands [89]Zr-nivolumab and [89]Zr-atezolizumab. They targeted programmed cell death-1 and programmed cell death ligand 1 and found feasibility in binding extracranial and intracranial targets [83, 84]. Targets on CD8+ T cells are also being evaluated. A novel radioligand, ^{18}F-clofarabine, the substrate for the enzyme deoxycytidine kinase that is overexpressed in CD8+ T cells, has shown promise for imaging the immune response in glioblastoma during immune-modulating treatment and is under investigation in humans [85].

Insights Into Brain Tumor Neuroinflammation From Imaging Genomics

Imaging genomics is another technique for assessing neuroinflammation. It entails development of imaging biomarkers of underlying tissue DNA and RNA patterns indicative of tumor biology or immune states. Imaging genomics is the study of the relation between imaging features and patterns of gene expression, genetic mutations, and protein modifications [86, 87]. Imaging genomics has begun to yield noninvasive biomarkers of molecular hallmarks and key biology of glioblastoma, including O^6-methylguanine-DNA methyltransferase (MGMT) methylation status, IDH1 mutation status, tumor subtype, and immunoreactivity [86, 88–90]. Analytic techniques now allow complex whole genomic analyses of samples based on computer-identified image spatial textures and advanced imaging elements [87, 91]. In one of the first imaging genomics reports that associated brain tumor immunotypes with image patterns, Cho et al. [92] completed radiogenomic profiling of 60 patients with glioblastoma. The study identified positive correlations of CD68 (TAMs), CSF1R (TAMs), CD33 (myeloid-derived suppressor cell), and CD4 (helper and regulatory T cells) with CBV and negative correlations of CD3e (helper and cytotoxic T cells) and CD49d with ADC. Imaging genomics remains an area with potential for influencing clinical care by bridging medical imaging and molecular tumor characteristics.

Conclusion

In the era of immunotherapy and precision oncology, a focus only on imaging of brain tumor growth in isolation is inadequate for developing predictive biomarkers and defining therapy-mediated neuroinflammation. To this end, MRI and PET characteristics of tumor-associated neuroinflammation are under active investigation. Results of preliminary work suggest that USPIO nanoparticle-enhanced MRI may be useful in identifying the macrophage or microglial component of brain tumors, particularly in patients with treatment-induced neuroinflammation. PET has promise for determining tumor and brain microenvironment antigen expression, quantifying drug delivery, and evaluating therapeutic efficacy. Future research directions include the use of novel PET radiotracers and MRI contrast agents combined with imaging genomic techniques to define and quantify the degree of neuroinflammatory components in the tumor microenvironment. Collectively, these efforts to predict and monitor personalized therapeutic efficacy by noninvasive neuroinflammation imaging will help bring precision oncology strategies to treatment of brain tumors and improve the lives of patients.

Acknowledgments

References

1. Weathers SS, Gilbert MR. Toward personalized targeted therapeutics: an overview. Neurotherapeutics 2017; 14:256–264 [PubMed: 27995437]

2. Iliff JJ, Wang M, Liao Y, et al. A paravascular pathway facilitates CSF flow through the brain parenchyma and the clearance of interstitial solutes, including amyloid β. Sci Transl Med 2012; 4:147ra111

3. Berghoff AS, Lassmann H, Preusser M, Höftberger R. Characterization of the inflammatory response to solid cancer metastases in the human brain. Clin Exp Metastasis 2013; 30:69–81 [PubMed: 22752508]

4. Berghoff AS, Ricken G, Widhalm G, et al. Tumour-infiltrating lymphocytes and expression of programmed death ligand 1 (PD-L1) in melanoma brain metastases. Histopathology 2015; 66:289–299 [PubMed: 25314639]

5. Quail DF, Joyce JA. The microenvironmental landscape of brain tumors. Cancer Cell 2017; 31:326–341 [PubMed: 28292436]

6. Brown NF, Carter TJ, Ottaviani D, Mulholland P. Harnessing the immune system in glioblastoma. Br J Cancer 2018; 119:1171–1181 [PubMed: 30393372]

7. Katz AM, Amankulor NM, Pitter K, Helmy K, Squatrito M, Holland EC. Astrocyte-specific expression patterns associated with the PDGF-induced glioma microenvironment. PLoS One 2012; 7:e32453 [PubMed: 22393407]

8. Brandao M, Simon T, Critchley G, Giamas G. Astrocytes, the rising stars of the glioblastoma microenvironment. Glia 2019; 67:779–790 [PubMed: 30240060]

9. Fitzgerald DP, Palmieri D, Hua E, et al. Reactive glia are recruited by highly proliferative brain metastases of breast cancer and promote tumor cell colonization. Clin Exp Metastasis 2008; 25:799–810 [PubMed: 18649117]

10. Zhang L, Zhang S, Yao J, et al. Microenvironment-induced PTEN loss by exosomal microRNA primes brain metastasis outgrowth. Nature 2015; 527:100–104 [PubMed: 26479035]

11. Ghajar CM, Peinado H, Mori H, et al. The perivascular niche regulates breast tumour dormancy. Nat Cell Biol 2013; 15:807–817 [PubMed: 23728425]

12. Lyle LT, Lockman PR, Adkins CE, et al. Alterations in pericyte subpopulations are associated with elevated blood-tumor barrier permeability in experimental brain metastasis of breast cancer. Clin Cancer Res 2016; 22:5287–5299 [PubMed: 27245829]

13. van Tellingen O, Yetkin-Arik B, de Gooijer MC, Wesseling P, Wurdinger T, de Vries HE. Overcoming the blood-brain tumor barrier for effective glioblastoma treatment. Drug Resist Updat 2015; 19:1–12 [PubMed: 25791797]

14. Charles N, Holland EC. The perivascular niche microenvironment in brain tumor progression. Cell Cycle 2010; 9:3012–3021 [PubMed: 20714216]

15. O'Carroll SJ, Kho DT, Wiltshire R, et al. Pro-inflammatory TNFα and IL-1β differentially regulate the inflammatory phenotype of brain microvascular endothelial cells. J Neuroinflammation 2015; 12:131 [PubMed: 26152369]

16. Das S, Marsden PA. Angiogenesis in glioblastoma. N Engl J Med 2013; 369:1561–1563 [PubMed: 24131182]

17. Lockman PR, Mittapalli RK, Taskar KS, et al. Heterogeneous blood-tumor barrier permeability determines drug efficacy in experimental brain metastases of breast cancer. Clin Cancer Res 2010; 16:5664–5678 [PubMed: 20829328]

18. Nduom EK, Yang C, Merrill MJ, Zhuang Z, Lonser RR. Characterization of the blood-brain barrier of metastatic and primary malignant neoplasms. J Neurosurg 2013; 119:427–433 [PubMed: 23621605]

19. Sarkaria JN, Hu LS, Parney IF, et al. Is the blood-brain barrier really disrupted in all glioblastomas? A critical assessment of existing clinical data. Neuro Oncol 2018; 20:184–191 [PubMed: 29016900]

20. Aspelund A, Antila S, Proulx ST, et al. A dural lymphatic vascular system that drains brain interstitial fluid and macromolecules. J Exp Med 2015; 212:991–999 [PubMed: 26077718]

21. Hambardzumyan D, Gutmann DH, Kettenmann H. The role of microglia and macrophages in glioma maintenance and progression. Nat Neurosci 2016; 19:20–27 [PubMed: 26713745]

22. Ginhoux F, Greter M, Leboeuf M, et al. Fate mapping analysis reveals that adult microglia derive from primitive macrophages. Science 2010; 330:841–845 [PubMed: 20966214]

23. Chen Z, Feng X, Herting CJ, et al. Cellular and molecular identity of tumor-associated macrophages in glioblastoma. Cancer Res 2017; 77:2266–2278 [PubMed: 28235764]

24. Bowman RL, Klemm F, Akkari L, et al. Macrophage ontogeny underlies differences in tumor-specific education in brain malignancies. Cell Rep 2016; 17:2445–2459 [PubMed: 27840052]

25. Klemm F, Maas RR, Bowman RL, et al. Interrogation of the microenvironmental landscape in brain tumors reveals disease-specific alterations of immune cells. Cell 2020; 181:1643–1660 [PubMed: 32470396]

26. Olson OC, Kim H, Quail DF, Foley EA, Joyce JA. Tumor-associated macrophages suppress the cytotoxic activity of antimitotic agents. Cell Rep 2017; 19:101–113 [PubMed: 28380350]

27. Aras S, Zaidi MR. TAMeless traitors: macrophages in cancer progression and metastasis. Br J Cancer 2017; 117:1583–1591 [PubMed: 29065107]

28. Andreou KE, Soto MS, Allen D, et al. Anti-inflammatory microglia/macrophages as a potential therapeutic target in brain metastasis. Front Oncol 2017; 7:251 [PubMed: 29164051]

29. Xue J, Schmidt SV, Sander J, et al. Transcriptome-based network analysis reveals a spectrum model of human macrophage activation. Immunity 2014; 40:274–288 [PubMed: 24530056]

30. DeNardo DG, Ruffell B. Macrophages as regulators of tumour immunity and immunotherapy. Nat Rev Immunol 2019; 19:369–382 [PubMed: 30718830]

31. Heimberger AB, Abou-Ghazal M, Reina-Ortiz C, et al. Incidence and prognostic impact of FoxP3+ regulatory T cells in human gliomas. Clin Cancer Res 2008; 14:5166–5172 [PubMed: 18698034]

32. Pardoll DM. The blockade of immune checkpoints in cancer immunotherapy. Nat Rev Cancer 2012; 12:252–264 [PubMed: 22437870]

33. Weinstein JS, Varallyay CG, Dosa E, et al. Superparamagnetic iron oxide nanoparticles: diagnostic magnetic resonance imaging and potential therapeutic applications in neurooncology and central nervous system inflammatory pathologies, a review. J Cereb Blood Flow Metab 2010; 30:15–35 [PubMed: 19756021]

34. Toth GB, Varallyay CG, Horvath A, et al. Current and potential imaging applications of ferumoxytol for magnetic resonance imaging. Kidney Int 2017; 92:47–66 [PubMed: 28434822]

35. McConnell HL, Schwartz DL, Richardson BE, Woltjer RL, Muldoon LL, Neuwelt EA. Ferumoxytol nanoparticle uptake in brain during acute neuroinflammation is cell-specific. Nanomedicine (Lond) 2016; 12:1535–1542

36. Ugga L, Romeo V, Tedeschi E, Brunetti A, Quarantelli M. Superparamagnetic iron oxide nanocolloids in MRI studies of neuroinflammation. J Neurosci Methods 2018; 310:12–23 [PubMed: 29913184]

37. Hamilton BE, Barajas R, Nesbit GM, et al. Ferumoxytol-enhanced MRI is not inferior to gadolinium-enhanced MRI in detecting intracranial metastatic disease and metastasis size. AJR 2020; 215:1436–1442 [PubMed: 33052739]

38. Hamilton BE, Nesbit GM, Dosa E, et al. Comparative analysis of ferumoxytol and gadoteridol enhancement using T1- and T2-weighted MRI in neuroimaging. AJR 2011; 197:981–988 [PubMed: 21940589]

39. Varallyay CG, Nesbit E, Fu R, et al. High-resolution steady-state cerebral blood volume maps in patients with central nervous system neoplasms using ferumoxytol, a superparamagnetic iron oxide nanoparticle. J Cereb Blood Flow Metab 2013; 33:780–786 [PubMed: 23486297]

40. Barajas RF Jr, Politi LS, Anzalone N, et al. Consensus recommendations for MRI and PET imaging of primary central nervous system lymphoma: guideline statement from the International Primary CNS Lymphoma Collaborative Group (IPCG). Neuro Oncol 2021; 23:1056–1071 [PubMed: 33560416]

41. Boxerman JL, Quarles CC, Hu LS, et al. Jumpstarting Brain Tumor Drug Development Coalition Imaging Standardization Steering Committee. Consensus recommendations for a dynamic susceptibility contrast MRI protocol for use in high-grade gliomas. Neuro Oncol 2020; 22:1262–1275 [PubMed: 32516388]

42. Ellingson BM, Bendszus M, Boxerman J, et al. ; Jumpstarting Brain Tumor Drug Development Coalition Imaging Standardization Steering Committee. Consensus recommendations for a standardized brain tumor imaging protocol in clinical trials. Neuro Oncol 2015; 17:1188–1198 [PubMed: 26250565]

43. Kaufmann TJ, Smits M, Boxerman J, et al. Consensus recommendations for a standardized brain tumor imaging protocol for clinical trials in brain metastases. Neuro Oncol 2020; 22:757–772 [PubMed: 32048719]

44. Barajas RF, Hamilton BE, Schwartz D, et al. Combined iron oxide nanoparticle ferumoxytol and gadolinium contrast enhanced MRI define glioblastoma pseudoprogression. Neuro Oncol 2019; 21:517–526 [PubMed: 30277536]

45. Thust SC, van den Bent MJ, Smits M. Pseudoprogression of brain tumors. J Magn Reson Imaging 2018; 48:571–589

46. Gahramanov S, Varallyay C, Tyson RM, et al. Diagnosis of pseudoprogression using MRI perfusion in patients with glioblastoma multiforme may predict improved survival. CNS Oncol 2014; 3:389–400 [PubMed: 25438810]

47. Barajas RF Jr, Chang JS, Segal MR, et al. Differentiation of recurrent glioblastoma multiforme from radiation necrosis after external beam radiation therapy with dynamic susceptibility-weighted contrast-enhanced perfusion MR imaging. Radiology 2009; 253:486–496 [PubMed: 19789240]

48. Barajas RF Jr, Cha S. Benefits of dynamic susceptibility-weighted contrast-enhanced perfusion MRI for glioma diagnosis and therapy. CNS Oncol 2014; 3:407–419 [PubMed: 25438812]

49. Hu LS, Eschbacher JM, Heiserman JE, et al. Reevaluating the imaging definition of tumor progression: perfusion MRI quantifies recurrent glioblastoma tumor fraction, pseudoprogression, and radiation necrosis to predict survival. Neuro Oncol 2012; 14:919–930 [PubMed: 22561797]

50. Iv M, Liu X, Lavezo J, et al. Perfusion MRI–based fractional tumor burden differentiates between tumor and treatment effect in recurrent glioblastomas and informs clinical decision-making. AJNR 2019; 40:1649–1657 [PubMed: 31515215]

51. van Dijken BRJ, van Laar PJ, Holtman GA, van der Hoorn A. Diagnostic accuracy of magnetic resonance imaging techniques for treatment response evaluation in patients with high-grade glioma, a systematic review and meta-analysis. Eur Radiol 2017; 27:4129–4144 [PubMed: 28332014]

52. Tsakiris C, Siempis T, Alexiou GA, et al. Differentiation between true tumor progression of glioblastoma and pseudoprogression using diffusion-weighted imaging and perfusion-weighted imaging: systematic review and meta-analysis. World Neurosurg 2020; 144:e100–e109 [PubMed: 32777397]

53. Suh CH, Kim HS, Jung SC, Choi CG, Kim SJ. Multiparametric MRI as a potential surrogate endpoint for decision-making in early treatment response following concurrent chemoradiotherapy in patients with newly diagnosed glioblastoma: a systematic review and meta-analysis. Eur Radiol 2018; 28:2628–2638 [PubMed: 29374321]

54. Okada H, Weller M, Huang R, et al. Immunotherapy response assessment in neuro-oncology: a report of the RANO working group. Lancet Oncol 2015; 16:e534–e542 [PubMed: 26545842]

55. U.S. FDA website. FDA drug safety communication: FDA strengthens warnings and changes prescribing instructions to decrease the risk of serious allergic reactions with anemia drug Feraheme (ferumoxytol). www.fda.gov/drugs/drug-safety-and-availability/fda-drug-safety-communication-fda-strengthens-warnings-and-changes-prescribing-instructions-decrease Published March 30, 2015. Accessed August 10, 2021

56. Nguyen KL, Yoshida T, Kathuria-Prakash N, et al. Multicenter safety and practice for off-label diagnostic use of ferumoxytol in MRI. Radiology 2019; 293:554–564 [PubMed: 31638489]

57. ACR Committee on Drugs and Contrast Media. ACR manual on contrast media. American College of Radiology website. www.acr.org/-/media/ACR/files/clinical-resources/contrast_media.pdf. Published 2021. Accessed August 12, 2021

58. Lim W, Afif W, Knowles S, et al. Canadian expert consensus: management of hypersensitivity reactions to intravenous iron in adults. Vox Sang 2019; 114:363–373 [PubMed: 30937914]

59. Iv M, Samghabadi P, Holdsworth S, et al. Quantification of macrophages in high-grade gliomas by using ferumoxytol-enhanced MRI: a pilot study. Radiology 2019; 290:198–206 [PubMed: 30398435]

60. Barajas RF Jr, Schwartz D, McConnell HL, et al. Distinguishing extravascular from intravascular ferumoxytol pools within the brain: proof of concept in patients with treated glioblastoma. AJNR 2020; 41:1193–1200 [PubMed: 32527840]

61. Narayanaswami V, Dahl K, Bernard-Gauthier V, Josephson L, Cumming P, Vasdev N. Emerging PET radiotracers and targets for imaging of neuroinflammation in neurodegenerative diseases: outlook beyond TSPO. Mol Imaging 2018; 17:1536012118792317 [PubMed: 30203712]

62. Papadopoulos V, Baraldi M, Guilarte TR, et al. Translocator protein (18kDa): new nomenclature for the peripheral-type benzodiazepine receptor based on its structure and molecular function. Trends Pharmacol Sci 2006; 27:402–409 [PubMed: 16822554]

63. Janczar K, Su Z, Raccagni I, et al. The 18-kDa mitochondrial translocator protein in gliomas: from the bench to bedside. Biochem Soc Trans 2015; 43:579–585 [PubMed: 26551696]

64. Zinnhardt B, Roncaroli F, Foray C, et al. Imaging of the glioma microenvironment by TSPO PET. Eur J Nucl Med Mol Imaging 2021 Mar 15 [published online]

65. Lavisse S, Guillermier M, Hérard AS, et al. Reactive astrocytes overexpress TSPO and are detected by TSPO positron emission tomography imaging. J Neurosci 2012; 32:10809–10818 [PubMed: 22875916]

66. Albrecht DS, Granziera C, Hooker JM, Loggia ML. In vivo imaging of human neuroinflammation. ACS Chem Neurosci 2016; 7:470–483 [PubMed: 26985861]

67. Su Z, Roncaroli F, Durrenberger PF, et al. The 18-kDa mitochondrial translocator protein in human gliomas: an 11C-(R)PK11195 PET imaging and neuropathology study. J Nucl Med 2015; 56:512–517 [PubMed: 25722450]

68. Zinnhardt B, Müther M, Roll W, et al. TSPO imaging-guided characterization of the immunosuppressive myeloid tumor microenvironment in patients with malignant glioma. Neuro Oncol 2020; 22:1030–1043 [PubMed: 32047908]

69. Zinnhardt B, Pigeon H, Thézé B, et al. Combined PET imaging of the inflammatory tumor microenvironment identifies margins of unique radiotracer uptake. Cancer Res 2017; 77:1831–1841 [PubMed: 28137769]

70. Ikawa M, Lohith TG, Shrestha S, et al. ; Biomarkers Consortium Radioligand Project Team. ^{11}C-ER176, a radioligand for 18-kDa translocator protein, has adequate sensitivity to robustly image all three affinity genotypes in human brain. J Nucl Med 2017; 58:320–325 [PubMed: 27856631]

71. Cumming P, Burgher B, Patkar O, et al. Sifting through the surfeit of neuroinflammation tracers. J Cereb Blood Flow Metab 2018; 38:204–224 [PubMed: 29256293]

72. Tang D, Li J, Nickels ML, Huang G, Cohen AS, Manning HC. Preclinical evaluation of a novel TSPO PET ligand 2-(7-Butyl-2-(4-(2-[18F]fluoroethoxy) phenyl)-5-methylpyrazolo[1,5-a]pyrimidin-3-yl)-N,N-diethylacetamide (18F-VUIIS1018A) to image glioma. Mol Imaging Biol 2019; 21:113–121 [PubMed: 29869061]

73. Albert NL, Unterrainer M, Fleischmann DF, et al. TSPO PET for glioma imaging using the novel ligand ^{18}F-GE-180: first results in patients with glioblastoma. Eur J Nucl Med Mol Imaging 2017; 44:2230–2238 [PubMed: 28821920]

74. Tran TT, Gallezot JD, Jilaveanu LB, et al. [^{11}C]Methionine and [^{11}C]PBR28 as PET imaging tracers to differentiate metastatic tumor recurrence or radiation necrosis. Mol Imaging 2020; 19:1536012120968669 [PubMed: 33147119]

75. Pannell M, Economopoulos V, Wilson TC, et al. Imaging of translocator protein upregulation is selective for pro-inflammatory polarized astrocytes and microglia. Glia 2020; 68:280–297 [PubMed: 31479168]

76. Balachandran S, Husain MM, Adametz JR, Pallin JS, Angtuaco TL, Boyd CM. Uptake of indium-111-labeled leukocytes by brain metastasis. Neurosurgery 1987; 20:606–609 [PubMed: 3587554]

77. Costa GL, Sandora MR, Nakajima A, et al. Adoptive immunotherapy of experimental autoimmune encephalomyelitis via T cell delivery of the IL-12 p40 subunit. J Immunol 2001; 167:2379–2387 [PubMed: 11490028]

78. Anderson SA, Shukaliak-Quandt J, Jordan EK, et al. Magnetic resonance imaging of labeled T-cells in a mouse model of multiple sclerosis. Ann Neurol 2004; 55:654–659 [PubMed: 15122705]

79. Price CJ, Menon DK, Peters AM, et al. Cerebral neutrophil recruitment, histology, and outcome in acute ischemic stroke: an imaging-based study. Stroke 2004; 35:1659–1664 [PubMed: 15155970]

80. Yaghoubi SS, Jensen MC, Satyamurthy N, et al. Noninvasive detection of therapeutic cytolytic T cells with 18F-FHBG PET in a patient with glioma. Nat Clin Pract Oncol 2009; 6:53–58 [PubMed: 19015650]

81. Keu KV, Witney TH, Yaghoubi S, et al. Reporter gene imaging of targeted T cell immunotherapy in recurrent glioma. Sci Transl Med 2017; 9:373.1

82. Shaffer TM, Aalipour A, Schürch CM, Gambhir SS. PET imaging of the natural killer cell activation receptor NKp30. J Nucl Med 2020; 61:1348–1354 [PubMed: 32532927]

83. Cole EL, Kim J, Donnelly DJ, et al. Radiosynthesis and preclinical PET evaluation of 89Zr-nivolumab (BMS-936558) in healthy non-human primates. Bioorg Med Chem 2017; 25:5407–5414 [PubMed: 28803798]

84. Bensch F, van der Veen EL, Lub-de Hooge MN, et al. [89]Zr-atezolizumab imaging as a non-invasive approach to assess clinical response to PD-L1 blockade in cancer. Nat Med 2018; 24:1852–1858 [PubMed: 30478423]

85. Antonios JP, Soto H, Everson RG, et al. Detection of immune responses after immunotherapy in glioblastoma using PET and MRI. Proc Natl Acad Sci USA 2017; 114:10220–10225 [PubMed: 28874539]

86. ElBanan MG, Amer AM, Zinn PO, Colen RR. Imaging genomics of glioblastoma: state of the art bridge between genomics and neuroradiology. Neuroimaging Clin N Am 2015; 25:141–153 [PubMed: 25476518]

87. Li ZC, Bai H, Sun Q, et al. Multiregional radiomics features from multiparametric MRI for prediction of MGMT methylation status in glioblastoma multiforme: a multicentre study. Eur Radiol 2018; 28:3640–3650 [PubMed: 29564594]

88. Carrillo JA, Lai A, Nghiemphu PL, et al. Relationship between tumor enhancement, edema, IDH1 mutational status, MGMT promoter methylation, and survival in glioblastoma. AJNR 2012; 33:1349–1355 [PubMed: 22322613]

89. Gutman DA, Cooper LA, Hwang SN, et al. MR imaging predictors of molecular profile and survival: multi-institutional study of the TCGA glioblastoma data set. Radiology 2013; 267:560–569 [PubMed: 23392431]

90. Narang S, Kim D, Aithala S, et al. Tumor image-derived texture features are associated with CD3 T-cell infiltration status in glioblastoma. Oncotarget 2017; 8:101244–101254 [PubMed: 29254160]

91. Barajas RF Jr, Hodgson JG, Chang JS, et al. Glioblastoma multiforme regional genetic and cellular expression patterns: influence on anatomic and physiologic MR imaging. Radiology 2010; 254:564–576 [PubMed: 20093527]

92. Cho HR, Jeon H, Park CK, Park SH, Choi SH. Radiogenomics profiling for glioblastoma-related immune cells reveals CD49d expression correlation with MRI parameters and prognosis. Sci Rep 2018; 8:16022 [PubMed: 30375429]

HIGHLIGHTS

- This article reviews the use of biologically specific noninvasive imaging biomarkers of brain tumor therapeutic monitoring and treatment-induced neuroinflammation.

- Delayed phase iron nanoparticle contrast-enhanced MRI can capture tumor-associated neuroinflammation, which may be indicative of therapeutic efficacy and clinical outcomes.

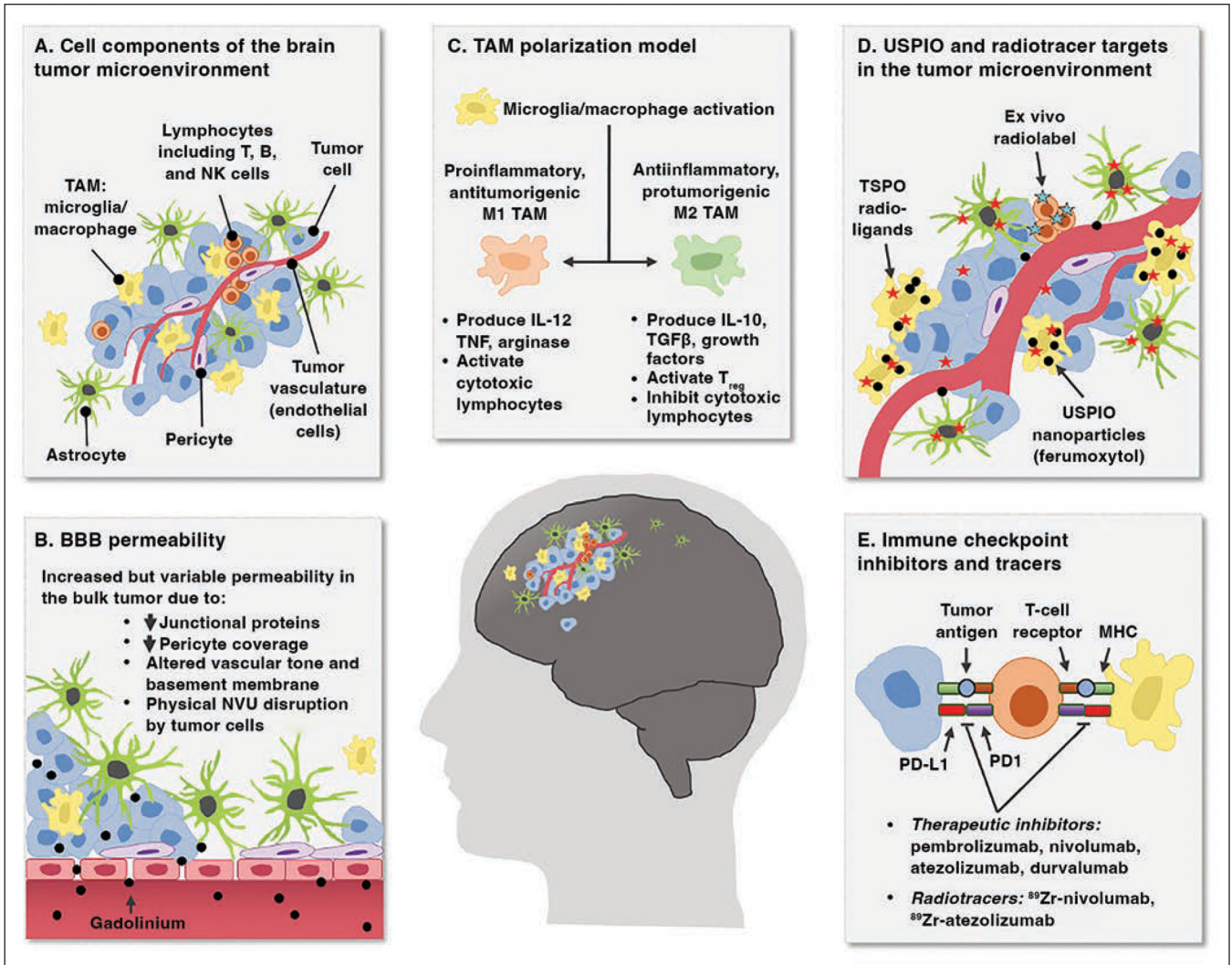- Immunologic PET tracers can be used to monitor the brain tumor–immune interface.

Fig. 1.

Chart shows neuroinflammation in brain tumor microenvironment presenting noninvasive imaging targets.

A, Cellular components of brain tumor microenvironment include milieu of resident and infiltrating cells, including neoplastic primary or metastatic tumor cells, lymphocytes, tumor-associated macrophages (TAMs), astrocytes, pericytes, and endothelial cells. NK = natural killer.

B, Blood-brain barrier (BBB) has variable permeability in brain tumors that is clinically visualized as intraparenchymal leakage of gadolinium contrast agent. NVU = neurovascular unit, ↓ = decreased.

C, TAMs in brain tumors can be differentially activated into proinflammatory and antiinflammatory reactive states that have opposing effects on tumor control and further propagate neuroinflammation through production and secretion of soluble immune-modulating factors. IL = interleukin, T_{reg} = regulatory T cells, TGFβ = transforming growth factor β, TNF = tumor necrosis factor.

D, Intravascularly delivered contrast agents and radioligands have potential for selective labeling of key immune elements of brain tumor microenvironment for noninvasive tracking. Specific expression and uptake distribution of these molecules is area of active investigation that is debated. USPIO = ultrasmall superparamagnetic iron oxide, TSPO = translator protein.

E, Immune checkpoints in brain tumor microenvironment are expressed by several cell types. Recent evidence suggests possible contribution of innate immune cell types. These checkpoints are target of multiple immunotherapies, and development of radiotracers to track their expression is underway. MHC = major histocompatibility complex, PD1 = programmed cell death 1, PD-L1 = programmed cell death ligand 1.
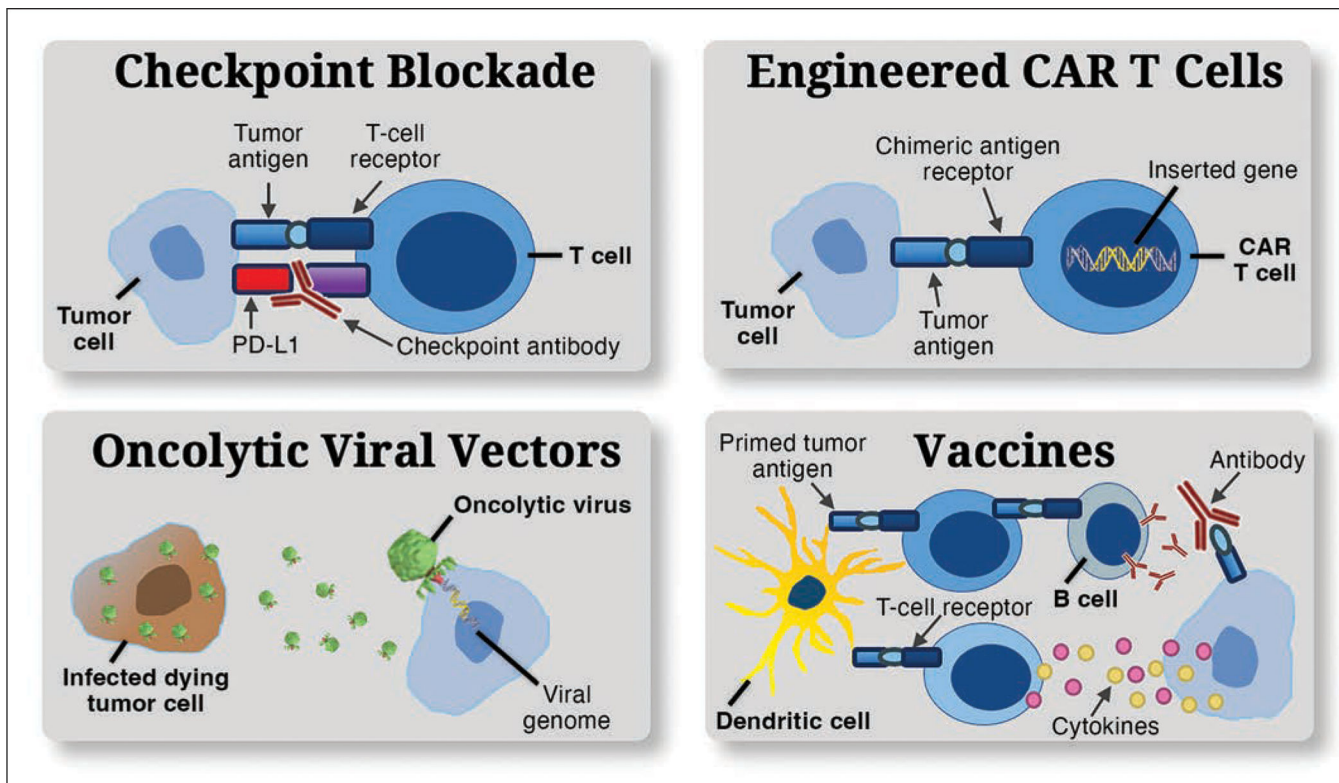
Fig. 2.
Charts show mechanisms of brain tumor immunotherapy. Various immunotherapeutic strategies have been developed to overcome tumor immune evasion and to reprogram dysregulated immune microenvironment as means of improving clinical outcomes. Checkpoint pathways (*top left*) play critical role in maintaining immune homeostasis by inhibiting cytotoxic T-cell efficacy, facilitating tumor immune evasion. This recognition led to development of monoclonal antibodies targeting these receptors. Disrupting checkpoint signaling unlocks cytotoxic T cell–mediated tumor cell killing, reduces numbers of regulatory T cells, and promotes proinflammatory cytokines within tumor bed. Use of immune checkpoint blockade has markedly improved overall survival in several solid tumors, including metastatic melanoma, leading to great interest in its use in glioblastoma. PD-L1 = programmed cell death ligand 1. Chimeric antigen receptor (CAR) T cells (*top right*) have gained wide use in therapy for various hemopoietic-based lymphomas and are emerging as potential therapeutic avenue in glioblastoma. CAR T cells are genetically modified to express CAR. This incorporates antigen-recognition moieties that endow autologous T cells with specificity against glioblastoma antigens, such as epidermal growth factor receptor variant III. Major area of therapeutic cancer research is construction of oncolytic viruses (*bottom left*) that not only target cancer cells but also retain their ability to infect, usurping host replication machinery and releasing newly made progeny to infect other transformed cells after lysing and killing host cell. One approach is to deliver therapeutic genes, such as inactivating mutation in thymidine kinase gene, via viral vector. Second approach is direct induction of tumor cell cytotoxicity. Both approaches subsequently present tumor antigen and potentiate adaptive immune response. In vaccine-

based immunotherapies (*bottom right*), tumor-associated antigens are used to train immune system to target tumor cells through various immune mechanisms in effort to induce cytotoxic tumor effects. Tumor antigens are presented to antigen-presenting immune cells, such as dendritic cells, ex vivo. These administered cells then induce potent adaptive immune stimulus against tumor.
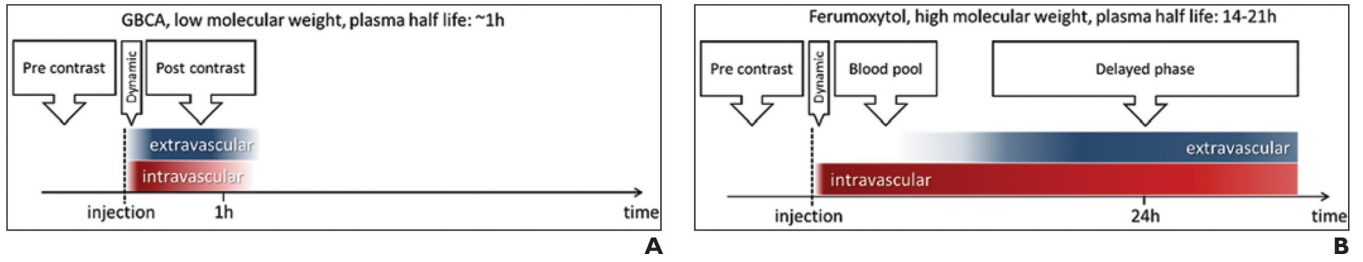
Fig. 3.
Chart shows phases of gadolinium-based contrast agent (GBCA) and iron nanoparticle (ferumoxytol) MRI changes in early and delayed phases of imaging. **A** and **B,** Unlike GBCAs (**A**), ferumoxytol (**B**) has long intravascular half-life that results in long blood pool phase before detectable contrast extravasation within brain tumor microenvironment. This facilitates dual assessment of GBCA and ferumoxytol T1-weighted enhancement characteristics for assessment of brain tumor–associated neuroinflammation. (Reprinted from *Kidney International*, 92, Toth GB, Varallyay CG, Horvath A, et al., Current and potential imaging applications of ferumoxytol for MRI, 47–66, Copyright [2017], www.sciencedirect.com/journal/kidney-international, with permission from International Society of Nephrology)
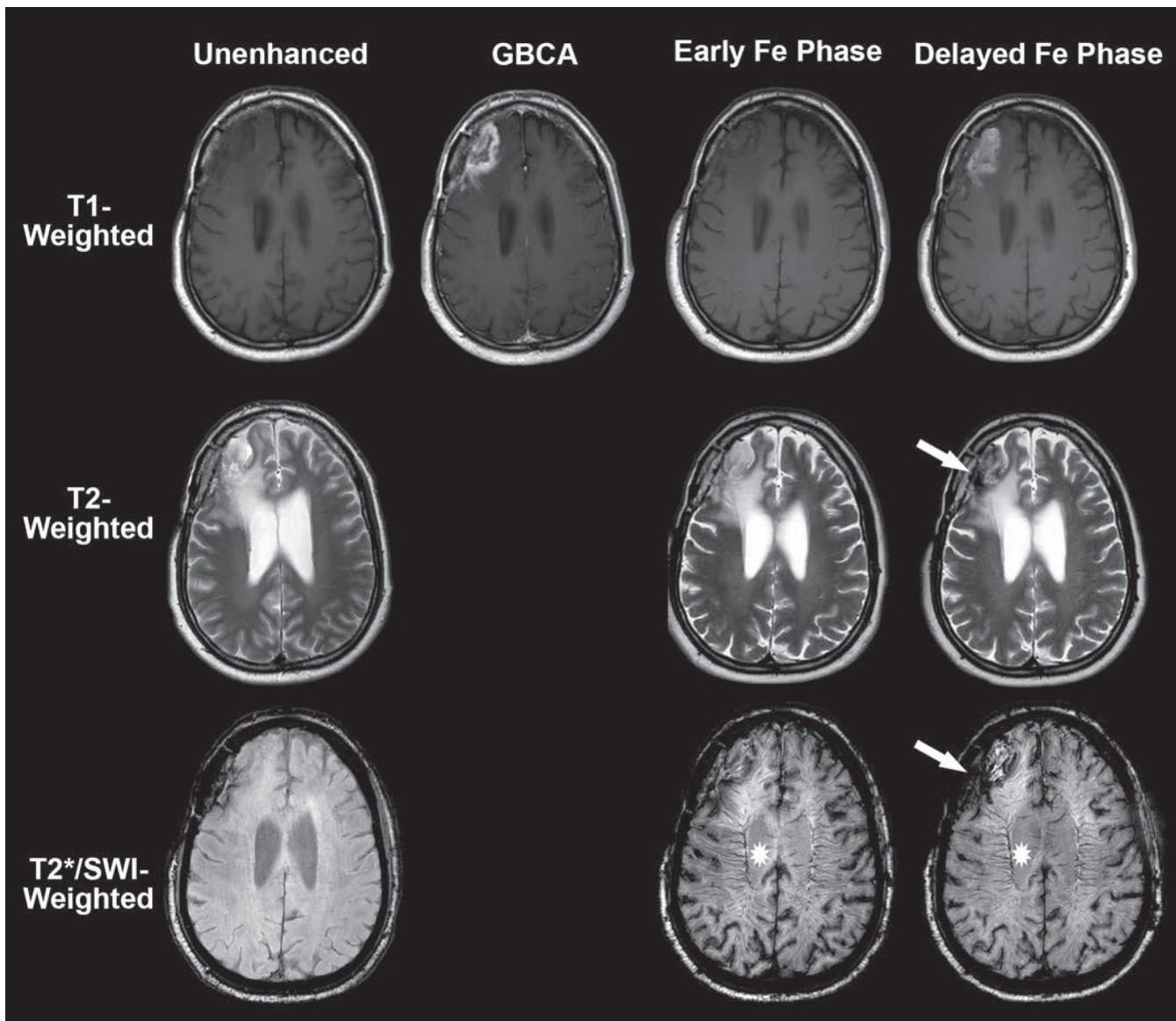
Fig. 4.
63-year-old man with recurrent metastatic lung cancer within right frontal lobe. Example of time-dependent signal changes observed with ferumoxytol-enhanced MRI. Baseline unenhanced MRI (*left*) shows T2-hyperintense mass with susceptibility along resection cavity margin and absence of intrinsic T1 shortening. Gadolinium-based contrast agent (GBCA)-enhanced T1-weighted image (*second from left*) shows typical masslike enhancement consistent with recurrent disease. Early intravascular phase ferumoxytol (Fe)-enhanced imaging (*second from right*) performed immediately after infusion shows negligible T1 and T2 change within brain parenchyma. However, T2*/susceptibility-weighted imaging (SWI) shows marked intravascular susceptibility effect (*star, second from right*) within cerebral vasculature. This forms basis for steady-state cerebral blood volume map calculation (not shown). Delayed extravascular phase ferumoxytol imaging (*right*) shows marked T1 shortening, similar to that with GBCA. This highlights noninferiority

of ferumoxytol as alternative contrast agent for detection of primary and metastatic brain parenchymal foci. T2-weighted image shows hypointensity (*arrow*) similar in distribution to that on T2*/SWI. Persistence of intravascular signal (*star, right*) in delayed phase contaminates assessment of brain parenchyma. This forms basis for segregation and extravascular localization of ferumoxytol (SELFI) map calculation (not shown).
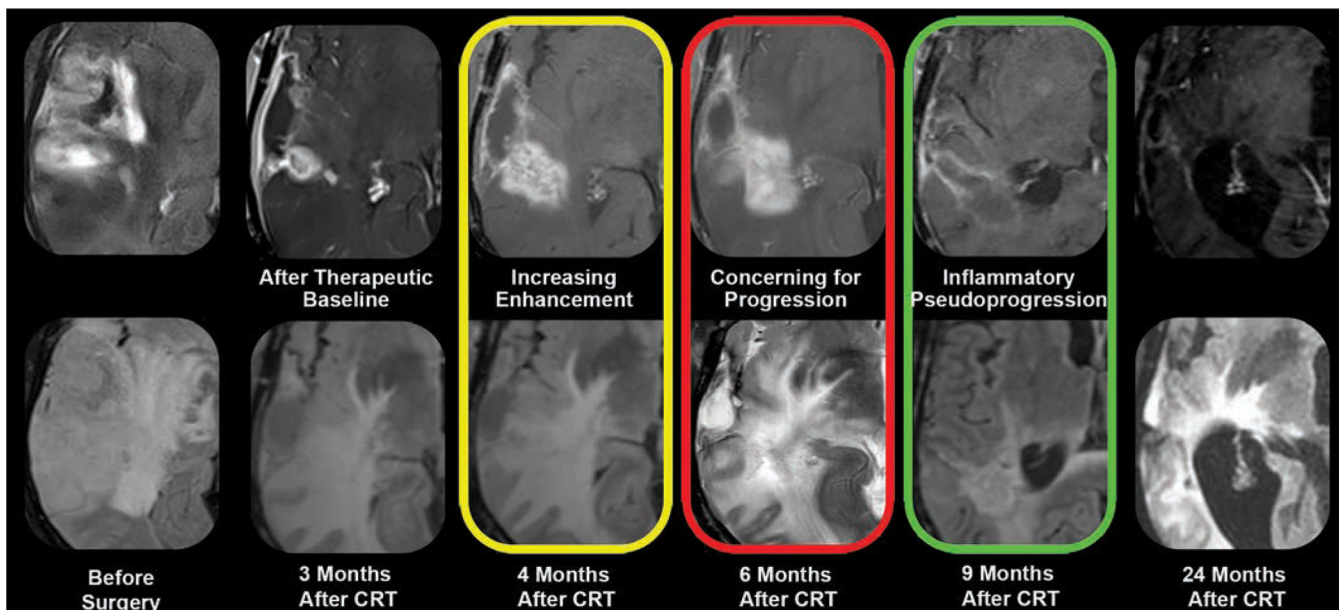
Fig. 5.
MRI appearance of glioblastoma neuroinflammatory pseudoprogression. Stupp protocol (chemoradiotherapy [CRT] and oral temozolomide) combined with fractionated external beam radiation therapy can induce neuroinflammation in patients with glioblastoma. Standard gadolinium-enhanced (*top row*) and T2-weighted/FLAIR (*bottom row*) morphologic MRI sequences, performed before and at multiple time points after CRT, are markedly limited for specifically defining therapy-induced neuroinflammatory changes. Both treatment failure and neuroinflammation manifest as enlarging enhancement and T2 hyperintensity (*yellow*, *red*). Unlike that of growing tumor, pseudoprogression enhancement spontaneously regresses and resolves without intervention (*green*). Retrospectively, this is diagnostic of neuroinflammation. However, response assessment in neurooncology criteria would not differentiate findings from those of growing tumor at height of inflammatory process (*red*), necessitating changes in therapy or biopsy. This exemplifies dilemma of monitoring pseudoprogression with gadolinium-based contrast agent, nonspecific biomarker of neurovascular unit integrity.
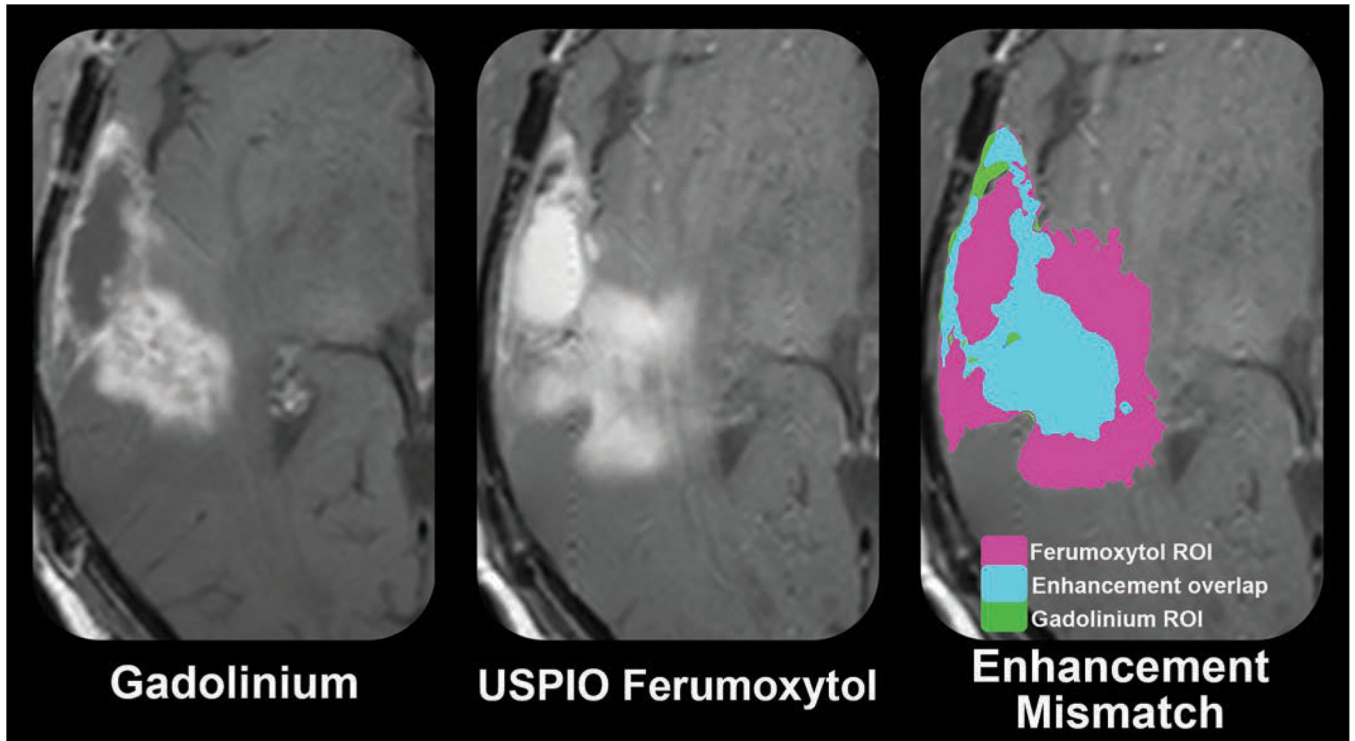
Fig. 6.

Ultrasmall superparamagnetic iron oxide (USPIO) ferumoxytol contrast enhancement may define glioblastoma neuroinflammatory pseudoprogression. Marked prominence of activated macrophage and microglia as cellular constituent of neuroinflammatory-mediated pseudoprogression has been impetus for investigating use of USPIO as biologically specific MRI metric. T1-weighted MR images show disproportionate enhancement (*right*) between USPIO ferumoxytol enhancement (*middle*) and gadolinium enhancement (*left*) in isocitrate dehydrogenase wild-type glioblastoma at time of presumed progression. Gadolinium-based contrast agent to ferumoxytol mismatch technique has shown preliminary promise in defining otherwise therapeutically induced neuroinflammation. Correlative histologic analysis with image-guided tissue sampling showed increased tumor-associated macrophage accumulation within regions of ferumoxytol enhancement.
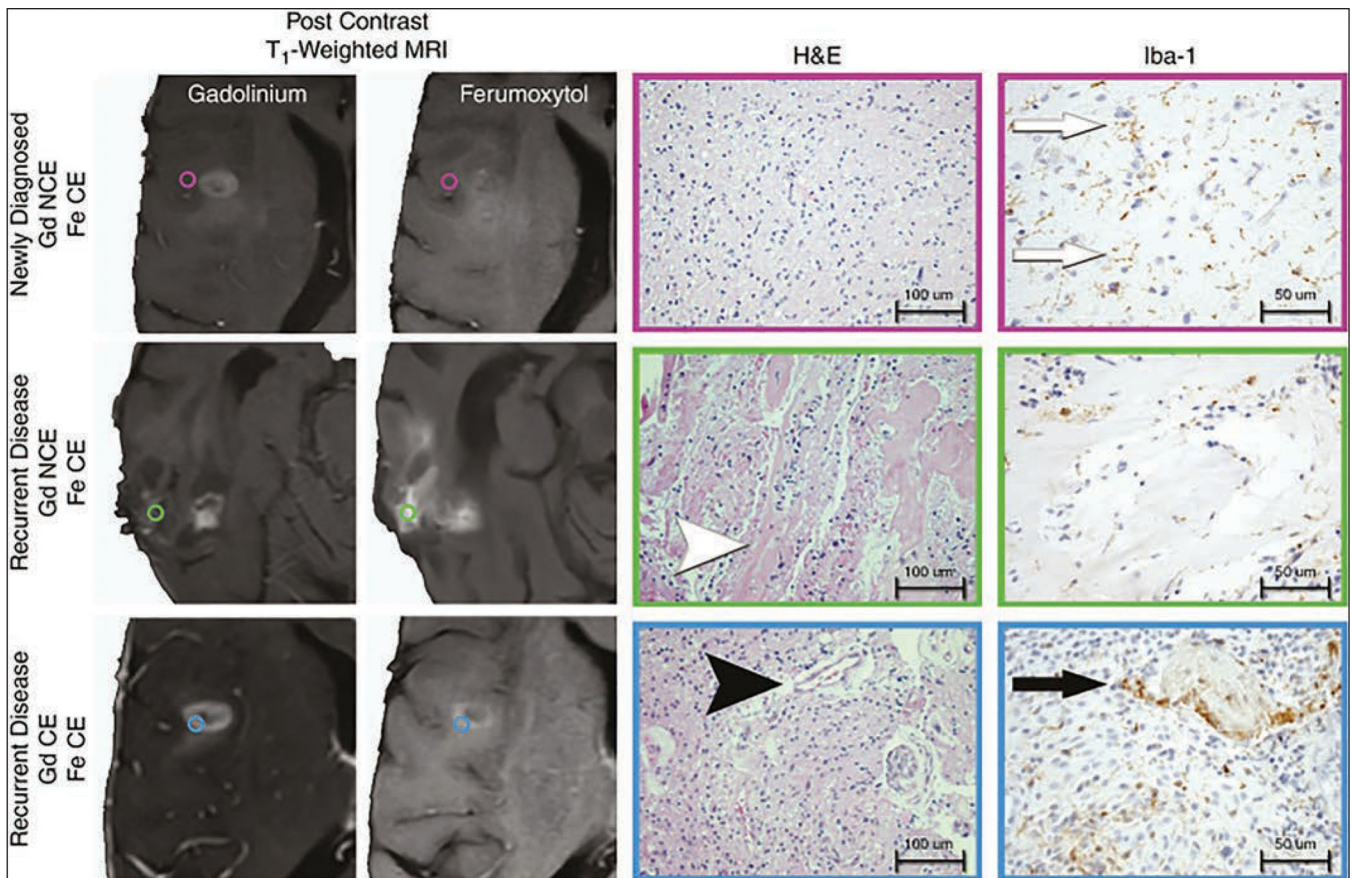
Fig. 7.

Histopathologic correlation of lesions enhancing after ferumoxytol (Fe)- and gadolinium (Gd)-based contrast agent administration in newly diagnosed and recurrent glioblastoma. Photomicrographs show regional image-guided tissue samples based on ferumoxytol and gadolinium contrast enhancement (CE) patterns. Standard-of-care stereotactic tissue sampling was performed in three patients with isocitrate dehydrogenase 1 (IDH1) wild-type glioblastoma at time of initial diagnosis or at time of disease recurrence. Tissue samples were classified by presence of gadolinium (*left*) or ferumoxytol (*second from left*) contrast enhancement. Tissue specimens were histopathologically characterized by presence of tumor and microvascular proliferation (H and E, ×20; 100-μm scale bar [*second from right*]) and presence of activated microglia or macrophages (ionized calcium-binding adapter molecule 1 [Iba1] stain, ×40; 50-μm scale bar [*right*]). Regions of ferumoxytol contrast enhancement but absence of gadolinium enhancement (NCE) were observed in patients with newly diagnosed glioblastoma (*purple, circles, top row*) and disease recurrence (*green, circles, middle row*). Ferumoxytol-only enhancing regions in patients with newly diagnosed IDH1 wild-type glioblastoma exhibited infiltrating glioma with low cellularity, delicate vasculature, and activated microglia (Iba1 brown-staining cells [*white arrows*]). Ferumoxytol-only enhancing regions in patients with recurrent IDH1 wild-type glioblastoma (*blue, circles, bottom row*) exhibited therapeutic changes evidenced by widespread vascular hyalinization (*white arrowhead*) with scattered macrophages without evidence of viable tumor. Dual contrast-enhancing sites (*bottom row*) appeared biologically similar in new

diagnosis and disease recurrence settings, being characterized by highly cellular tumor with microvascular proliferation (*black arrowhead*) and tumor-associated macrophages with epithelioid appearance (*black arrow*). (Reprinted from [44] and in public domain)
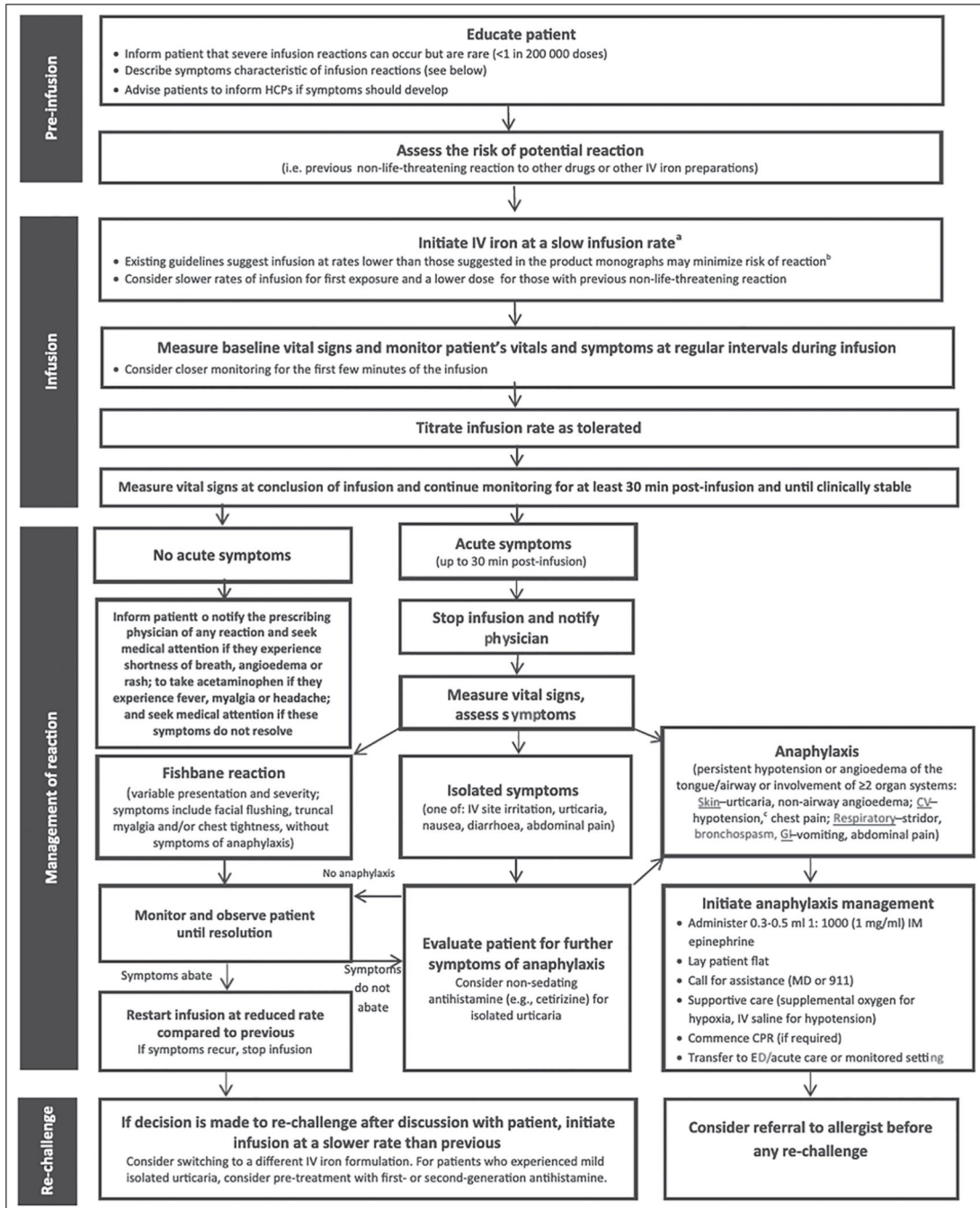
Fig. 8.

Chart shows potential hypersensitivity reaction management algorithm for IV iron administration. [a]Infusions should be conducted at site where personnel and resuscitative interventions are immediately available for treatment of severe hypersensitivity reactions. [b]Refer to product monograph for recommended rates of infusion. [c]Hypotension defined as 30 mm Hg decrease in systolic blood pressure (SBP) from baseline or SBP < 90 mm Hg. HCP = health care professional, CV = cardiovascular, GI = gastrointestinal, IM = intramuscular, MD = physician, CPR = cardiopulmonary resuscitation, ED =

emergency department. (Reprinted from Lim W, Waqqas Afif W, Knowles S, et al., doi.org/10.1111/vox.12773, 2019, subject to terms and including disclaimer in Section 5 of Creative Commons Attribution-NonCommercial License, creativecommons.org/licenses/by-nc/4.0/legalcode)

TABLE 1:

Delayed-Phase Ferumoxytol-Enhanced Neuroinflammatory MRI Protocol at 3 T

Characteristic	SWI[a]	T2-Weighted[a]	Contrast-Enhanced T1-Weighted[a,b,c]
Sequence	GRE	GE-EPI	TSE[d]
Plane	Axial	Axial	Any
Mode	3D	3D	3D
TR (ms)	26	> 2500	550–750
TE (ms)	20	80–120	Minimum
Inversion time (ms)	NA	NA	NA
Flip angle (°)	15	90/ 160	Default[e]
Matrix size			
Frequency	256	256	256
Phase	256	256	256
No. of excitations	1	1	1
FOV (mm)[f]	210	240	256
Slice thickness (mm)	1	1	1
Interslice spacing (mm)	0	0	0
Other options	T2*-weighted sequence may be substituted but provides lower spatial resolution	NA	Consider fat saturation
Parallel imaging factor[g]	Up to 2	Up to 2	Up to 2
Estimated acquisition time (min)[h]	5–8	5–8	5–8

Note—Listed sequences are performed 24–48 hours after ferumoxytol contrast injection. Brain tumor imaging protocol–compliant MRI with gadolinium-based contrast agent performed before ferumoxytol infusion allows assessment of baseline T1 shortening, presence of SWI/T2* susceptibility, and gadolinium enhancement characteristics and allows calculation of ferumoxytol-based cerebral blood volume (CBV) and segregation and extravascular localization of ferumoxytol imaging (SELFI) maps. Ferumoxytol and gadolinium administration can occur within the same MRI examination because the times of brain parenchymal signal changes are dissimilar for the two agents. The dose of ferumoxytol depends on the clinical scenario. However, in the context of brain tumor neuroinflammation, a dose of 4–7 mg/kg (up to a total dose of 510 mg) provides for calculation of ferumoxytol-based CBV and SELFI maps and assessment of delayed enhancement on T1-weighted images. Ferumoxytol should be administered in a 1:4 ratio diluted with normal saline solution over 15 minutes. The patient should be observed for 30 minutes for contrast reaction. Ferumoxytol should be administered only when personnel and therapies are immediately available for the treatment of anaphylaxis and other hypersensitivity reactions. SWI = susceptibility-weighted imaging, GRE = gradient-recalled echo, GE-EPI = gradient-echo echo-planar imaging, TSE = turbo spin-echo, NA = not applicable. (Information derived from [40])

[a]Contrast-enhanced images should be obtained with parameters equivalent to those for unenhanced images.

[b]TSE (Siemens Healthineers and Philips Healthcare) is equivalent to fast spin-echo (FSE; GE Healthcare, Hitachi, Toshiba Medical Systems).

[c] Obtained 24–48 hours after ferumoxytol contrast injection. Timing should be consistent across all MRI examinations.

[d] Acceptable 3D T1-weighted TSE sequences include CUBE (GE Healthcare), SPACE (Siemens Healthineers), VISTA (Philips Healthcare), isoFSE (Hitachi), and 3D MVOX (Canon Medical Systems).

[e] Flip angles for 3D TSE sequences (including CUBE and SPACE) are complicated because many use variable flip angle refocusing radiofrequency pulses to produce the desired image contrast. Investigators are encouraged to work with their vendors to determine the ideal parameters.

[f] As cited in prior consensus guidelines [40].

[g] Investigators are encouraged to work with their vendors to determine the best parallel imaging strategies, which may include simultaneous multislice imaging, controlled aliasing in parallel imaging resulting in higher acceleration, integrated parallel acquisition technique, GRAPPA, and turbo or other acceleration factors. High-performance MRI systems may be capable of higher acceleration factors.

[h] Imaging times provided are estimates only. Exact imaging times depend on individual MRI system and hardware performance capabilities.